Research article

A continuous peptide epitope reacting with pandemic influenza AH1N1 predicted by bioinformatic approaches

Jonathan P. Carrillo-Vazquez[a], José Correa-Basurto[b], Jazmin García-Machorro[c], Rafael Campos-Rodríguez[d], Violaine Moreau[e], Jorge L. Rosas-Trigueros[f], Cesar A. Reyes-López[a], Marlon Rojas-López[g] and Absalom Zamorano-Carrillo[a]*

Computational identification of potential epitopes with an immunogenic capacity challenges immunological research. Several methods show considerable success, and together with experimental studies, the efficiency of the algorithms to identify potential peptides with biological activity has improved. Herein, an epitope was designed by combining bioinformatics, docking, and molecular dynamics simulations. The hemagglutinin protein of the H1N1 influenza pandemic strain served as a template, owing to the interest of obtaining a scheme of immunization. Afterward, we performed enzyme-linked immunosorbent assay (ELISA) using the epitope to analyze if any antibodies in human sera before and after the influenza outbreak in 2009 recognize this peptide. Also, a plaque reduction neutralization test induced by virus-neutralizing antibodies and the IgG determination showed the biological activity of this computationally designed peptide. The results of the ELISAs demonstrated that the serum of both prepandemic and pandemic recognized the epitope. Moreover, the plaque reduction neutralization test evidenced the capacity of the designed peptide to neutralize influenza virus in Madin-Darby canine cells. Copyright © 2015 John Wiley & Sons, Ltd.

Additional supporting information may be found in the online version of this article at the publisher's web site.

Keywords: Peptide, Influenza, Bioinformatic

INTRODUCTION

The study of viral infectious diseases is of interest in the public health of any community. Molecular basis and new technologies are investigated and developed to improve the diagnostic and treatment of these pathologies, requiring a considerable financial resource to reach results [1]. Influenza virus has been considered as the primary cause of severe flu, which is 15% of all cases worldwide [2]. High mortality rates produced by antigenic variation make the control of this illness difficult [3]. Influenza, transmitted by a negative single-stranded virus, presents antigenic drift and antigenic shift, resulting in epidemics and pandemics [4]. Currently, vaccine development for influenza is related to the search for a method or a group of methods to discover a universal epitope that allows a more comprehensive immunization [5,6]. Many epitopes and sequences of distinct influenza virus strains have been reported, and various arise from the viral surface proteins [7–9]. These proteins are the best source of epitope data because they are localized in the most external part of a viral particle, participating in the process of viral adhesion into the host cell [10]. The influenza virus has four surface proteins. Two of them, M1 and M2, are in the inner part of the particle and include the most conserved sequences of amino acids [11,12]. The others, hemagglutinin (HA) and neuraminidase (NA), exhibit the highest antigenic variation of all influenza proteins and confer antigenic exposure to the immune cells of the host during the

* Correspondence to: A. Zamorano-Carrillo, Laboratorio de Bioquímica y Biofísica Computacional, Doctorado en Biotecnología, ENMH—IPN, Mexico, D.F., Mexico.
E-mail: absalomz2002@gmail.com

a   J. P. Carrillo-Vazquez, C. A. Reyes-López, A. Zamorano-Carrillo
Laboratorio de Bioquímica y Biofísica Computacional, Doctorado en Biotecnología ENMH—IPN, Mexico, D.F., Mexico

b   J. Correa-Basurto
Laboratorio de Modelado Molecular y Diseño de Fármacos, Escuela Superior de Medicina—IPN, Mexico, D.F., Mexico

c   J. García-Machorro
Laboratorio de Medicina de Conservación, Escuela Superior de Medicina—IPN, Mexico, D.F., Mexico

d   R. Campos-Rodríguez
Laboratorio de Inmunología Molecular, Escuela Superior de Medicina—IPN, Mexico, D.F., Mexico

e   V. Moreau
CNRS FRE 3009, SysDiag, CAP DELTA, Montpellier, France

f   J. L. Rosas-Trigueros
Laboratorio Transdisciplinario de Investigación en Sistemas Evolutivos SEPI-ESCOM-IPN, Mexico, D.F., Mexico

g   M. Rojas-López
Centro de Investigación en Biotecnología Aplicada—IPN, Tlaxcala, Mexico

entrance of the virus [13–15]. Mainly, HA exhibits four antigenic sites known as Ca, Cb, Sa, and Sb (Figure 1A and B) [16–18].

Some theoretical and experimental methods identify epitopes that can be the initial candidates for peptide vaccine design or new targets for molecular diagnosis [19–21]. Computational tools used for the prediction of epitopes include theoretical understanding of molecular interactions [22,23]. Bioinformatics research has developed mainly two strategies to predict epitopes: structural-based [24,25] and sequence-based predictors [26–28]. In the former, the search is focused on three-dimensional (3D) structure information [29,30], whereas the second strategy uses sequences related to immunogenicity. Both strategies depend on the content of databases with theoretical and experimental information where individual epitopes or sequences have been described as antigenic or immunogenic. Some tools also use the information of epitopes capable of being recognized by the major histocompatibility complex (MHC) class II. However, this addition to these methods of prediction remains an open problem because of the difficulty to predict T-cell responses [31,32]. Also, a problem lies in the epitopes mimicked by synthetic peptides because a sequence size of 6–10 residues is needed for antigen reactivity; nevertheless, they have been studied extensively in animal models with various results [33,34].

Usually, promising results have the potential to not only decrease costs but also avoid unwanted responses that occur with vaccines derived from attenuated live or killed pathogens [35,36]. In this work, we identify an epitope of the H1N1 human influenza strain through combining bioinformatic tools such as structural and sequential epitope predictors. Furthermore, docking and molecular dynamics (MD) simulations were used to analyze the interaction between the epitope and the MHC II molecule [37,38]. These bioinformatic simulations suggest how the peptide interacts with the pockets of the recognition groove of the MHC molecule and give information that could be useful for rational vaccine design. As a case for studying, we predicted a highly immunogenic continuous epitope of HA of the influenza strain AH1N1 2009 [39–41]. Additionally, as an experimental counterpart, a plaque reduction neutralization test (PRNT) induced by virus-neutralizing antibodies was performed to evaluate the peptide functionality.

Results

3D model selection of the HA of the human influenza H1N1

In early 2009, Di and coworkers reported a homology model of the HA H1N1 influenza strain and predicted some epitopes by SEPPA (Shanghai, China) program [25]. Later, in 2010, Xu and coworkers reported the crystallographic coordinates of influenza HA trimer with a Protein Data Bank (PDB) code 3LZG [42]. Although both 3D models show high similarity, in this work, we used 3LZG and its corresponding protein sequence.

Prediction of the epitope

Two epitope prediction methods were used, that is, sequence-based and structure-based predictors. Structural predictors, according to their strategy, localize more exposed sequences of amino acids and discard epitopes in hidden domains. Likewise, epitopes located in α-helix and β-folded regions were discarded because, despite these regions having less mobility, they could be difficult to recognize by the MHC and usually are hidden inside the protein. In contrast, loops or tails are more recognizable and become accommodated in the corresponding pockets by the MHC molecule because of their flexibility. Furthermore, these
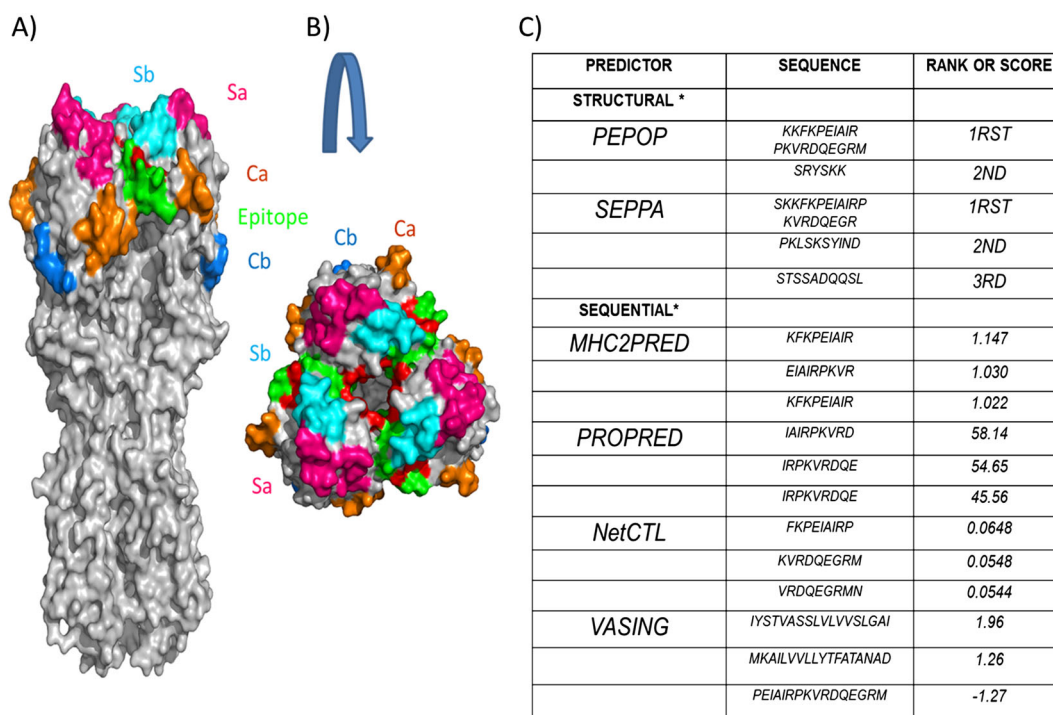

PREDICTOR	SEQUENCE	RANK OR SCORE
STRUCTURAL *		
PEPOP	KKFKPEIAIR PKVRDQEGRM	*1RST*
	SRYSKK	*2ND*
SEPPA	SKKFKPEIAIRP KVRDQEGR	*1RST*
	PKLSKSYIND	*2ND*
	STSSADQQSL	*3RD*
SEQUENTIAL*		
MHC2PRED	KFKPEIAIR	*1.147*
	EIAIRPKVR	*1.030*
	KFKPEIAIR	*1.022*
PROPRED	IAIRPKVRD	*58.14*
	IRPKVRDQE	*54.65*
	IRPKVRDQE	*45.56*
NetCTL	FKPEIAIRP	*0.0648*
	KVRDQEGRM	*0.0548*
	VRDQEGRMN	*0.0544*
VASING	IYSTVASSLVLVVSLGAI	*1.96*
	MKAILVVLLYTFATANAD	*1.26*
	PEIAIRPKVRDQEGRM	*-1.27*

Figure 1. Antigenic sites of HA and scores obtained from computational epitope predictors. (A) Three-dimensional representation of the HA trimer by Xu and coworkers. The antigenic sites of the HA highlighted in colors Sa, Sb, Ca, and Cb. The localization of the epitope predicted by PEPOP and its core are highlighted in green and red, respectively. (B) Superior view of the globular head of the HA trimer. (C) Rankings or scores of the sequence predicted according to the scale in the context of each software predictor.

structures were considered for the structural modeling of the immunogenic peptide [43,44]. The first system of prediction used was that implemented in the PEPOP server, and its results were compared with the other predictors (Figure 1C). PEPOP played the role of the initial reference because of its several features (length, amino acids, beta-turns, and hydrophobicity) that filter and refine the epitope search for the best structural prediction. In this initial approach, three more conditions were required: high score for MHC II recognition, presence of the epitope in a conserved region, and at the same time belonging to a structurally exposed domain. Therefore, we submitted into the PEPOP server two main chains, those corresponding to the HA trimer retrieved from 3LZG. A 20-residue-length epitope was requested to obtain a domain that could be recognized or processed by the immune system, in particular, by the MHC II [45–47]. Several amino acid sequences were predicted; however, owing to the absence of scientific reports and to our knowledge about these sequences, the epitope sequence KKFKPEIAIRPKVRDQEGRM (211–230 of chain A) was selected. The interest for this epitope is also due to it being located in the globular head of the HA. This surface portion is near a Ca2 antigenic site and includes the receptor binding region (Figure 1A and B) [48]. Also, it is known that residue 225 affects the receptor binding specificity of avian and human H1N1 viruses [49]. The epitope prediction presents a core of 10 amino acids (EIAIRPKVRD); according to the score of the PEPOP software, these represent the highest content of immunogenicity. When we compared the result of PEPOP with the other predictors, this sub-sequence (core) was also preferred by the epitope–MHC II and epitope–B cell predictors (Figure 1C).

A characterization of the predicted peptide was performed by the Peptide Property Calculator program (www.genscript.com/ssl-bin/site2/peptide_calculation.cgi), showing that its sequence has 40% hydrophobicity, 50% hydrophilicity, 15% acidic composition, and 35% basic composition. These proportions are essential for the peptide because they are related to immunogenicity [50,51]. The corresponding sequence of the epitope was submitted to a Protein–Protein Basic Local Alignment Search and Position-specific Iterated Basic Local Alignment Search (http://blast.ncbi.nlm.nih.gov/), resulting in it having a complete identity (100%) with a human protein related to a methyl-CpG-binding group (UNIPROT code: Q8WWY6) [52]. This protein is localized to the nucleus and restricted to the round spermatids in the postmeiotic stages of the male germ cell development. The score for identity was 100% only in the residues KVRDQEGR, and in the rest of the BLAST, alignments showed less than 90% of identity because of gaps. It is worthy to mention that the predicted epitope might not induce an autoimmune response because the methyl-CpG-binding trait is confined to the nucleus.

Docking and MD simulations of the peptide with the MHC class II

Three-dimensional models of the peptides and MHC II were used to describe the interactions between them by docking studies with AutoDock 4.0.1 (focused) and blind docking with CLUSPRO program [53,54]. The CLUSPRO program depicts free energy of the molecular interaction between the peptides and MHC II as the best free energy values (data not shown). The results demonstrate that the epitope predicted by PEPOP can be bonded by the MHC II recognition groove, with blind or restricted docking. A characteristic of docking is that the target, in this case MHC II, neglects the flexibility and the explicit solvent effects [55].

Therefore, from a complex obtained by AutoDock, MD simulations for 100 ns were performed to refine the epitope–MHC II complex with GROMACS [56–59]. To describe the epitope–MHC II interactions, we focused on the epitope recognition by the well-known MHC II pockets (P1, P4, P6, P7, and P9) located inside the recognition groove (Figure 2A). These regions participate in the formation of the epitope–MHC II complex necessary for the antigen presentation, and MD simulations provided evidence that the epitope reaches all MHC pockets [46,47]. The last structure reached by the MD simulations shows some changes in all the pockets, especially in P1 and P4. Also, during the simulations, Lys1 approaches the P1 (Gly86 in chain B) rapidly, although it interacts with residues nearby the P4 (Cys79 and Arg80 in chain B). Lys2, with less mobility, also interacts with P4; in particular, sharing with the Lys1 an interaction with the Cys79 (data not shown). Phe3 plays an interesting role because, during MD simulation, it interacts with residue of both chains Ile8 (chain A) and His13 (chain B, P4), suggesting that hydrophobic and polar amino acids play a significant role in antigen processing. Also, the interaction formed by Tyr78 (chain B, P4) and Arg10 was evidenced as stabilizing. Regarding P6 and P7, the Val65 (chain A) and Leu67 (chain B) were nearby Glu6 and Arg19, respectively (Figure 2).

To examine the epitope–MHC II complex interactions during the MD simulations, we analyzed the root mean square deviation (RMSD) and root mean square fluctuation (RMSF) values (Figure 3). The RMSD analysis showed that the model reaches convergence approximately at 20 ns and remains stable during the rest of the MD simulation (100 ns) (Figure 3A) [60–62]. Also, the RMSF values were retrieved from the three chains of the complex (chain A spanning from 4 to 181, B from 2 to 190, both of the MHC II, and C corresponding to 20 of the peptides) (Figure 3B and C). The MHC II was analyzed in each chain; chain A shows many long movements in a region, spanning from residues 30 to 60, that involves the pocket 1 and the initial part of the pocket 6. The RMSF values studied from chain B have first pick; this phenomenon was due to the flexibility of the amino acids in the amino-terminal region (residues 2, 3, and 4). Other regions present a local maximum because of the lack of some amino acids in the chain; this gap spans from residues 105 to 113 of chain B. The chain B residues that were involved in long movements were from the region near pockets 1, 7, and 9 (Figure 2B). The RMSF values show that the Phe3 of the peptide is the only amino acid that has limited movements compared with the rest of the peptide. The limited changes are due to the interaction of P1 and especially P4 with the His13, which is one of the unique binding residues of the P4. All the rest of the residues have variable movements, but when the complex achieves convergence, the residues become more limited in their movements (Figure 3C).

Design of the peptides

The peptide was revised to explore the versatility of the epitope in order to improve it by editing its residue sequence according to the literature and the analysis *in silico* [63–65]. The epitope predicted was modified to reduce its possible autoimmune response due to its complete homology with a human protein related to spermatogenesis. These modifications included the removal of the last five residues that belong to the homology region of the protein related to a methyl-CpG-binding group (KKFKPEIAIRPKVRDQEGRM). The second modification obeys the MD simulations results where the amino-terminal region showed
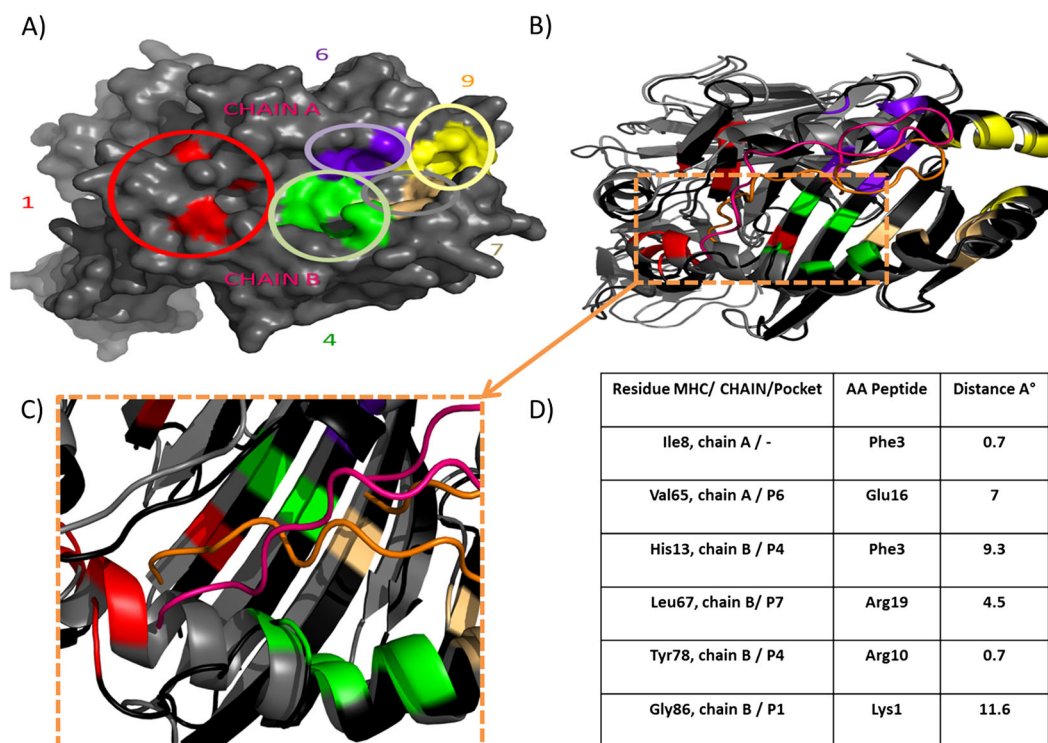
Residue MHC/ CHAIN/Pocket	AA Peptide	Distance A°
Ile8, chain A / -	Phe3	0.7
Val65, chain A / P6	Glu16	7
His13, chain B / P4	Phe3	9.3
Leu67, chain B/ P7	Arg19	4.5
Tyr78, chain B / P4	Arg10	0.7
Gly86, chain B / P1	Lys1	11.6

Figure 2. Pockets of the MHC and their interaction with the epitope. (A) Three-dimensional surface representation of the MHC molecule, circled and highlighted in color the pockets that involve the interaction with the epitope predicted by PEPOP (*P1* = red, *P4* = green, *P6* = blue, *P7* = light orange and *P9* = yellow). (B) Superposition of the final docking map (gray) and the 100 ns simulation (black). (C) Zoom near the pockets 1 and 4 of the recognition groove. (D) Distances obtained by a contact map analysis, some of these interactions are with specific amino acids of the pockets 1, 4, 6, and 7.
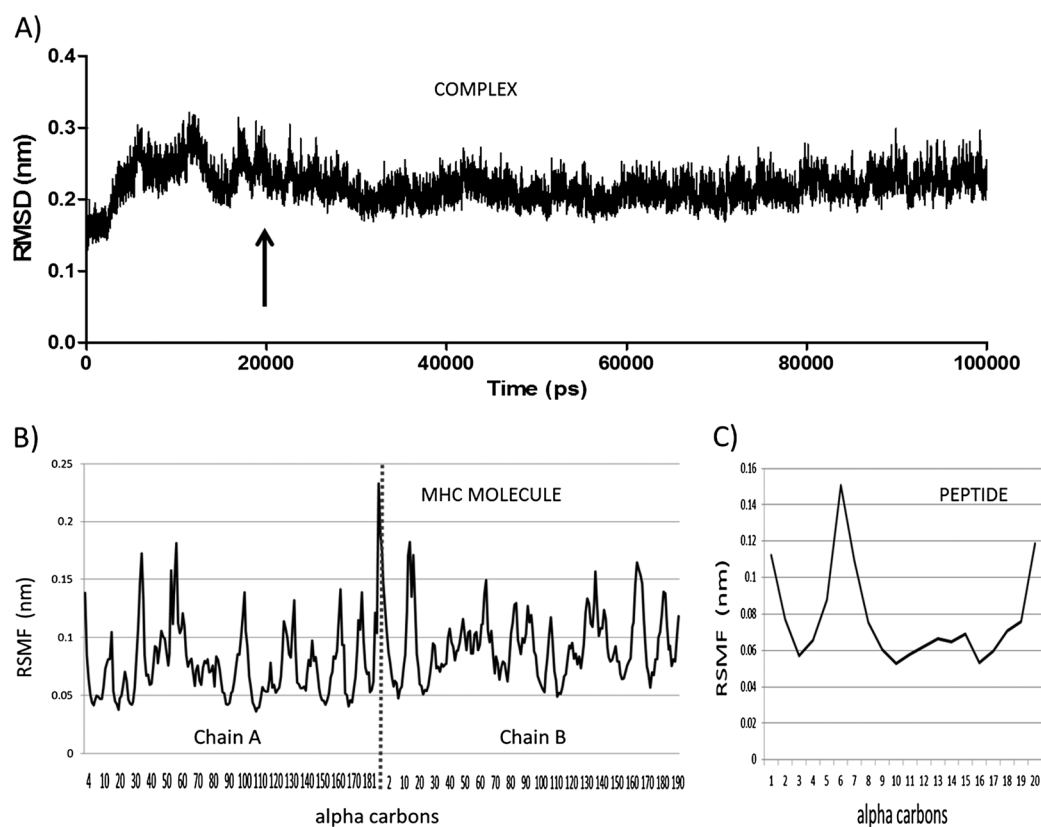

Figure 3. RMSD and RMSF parameters. (A) RMSD of the complex. (B) RMSF of the two chains of the MHC molecule. (C) Epitope of 20 amino acids.

a better interaction with the recognition groove. This result coincides with the report of Yano and coworkers, where it is mentioned that the KK linker sequence is preferred by cathepsin B to process antigens [66]. Thus, it is also consistent with the presence of the Lys1 and Lys2 in the amino-terminal region of the peptide; therefore, these residues remained unchanged. We named this peptide as p1 (KKFKPEIAIRPKVRD). The second peptide called peptide 2 (p2) conserves the sequence of p1 with an additional cysteine at the amino-terminal that functions as a linker for hemocyanin (KLH) [67]. This modification will provide evidence of the importance of the amino-terminal lysines (KLH-C-KKFKPEIAIRPKVRD). Another sequence of interest is RGD because it is preferred by the antigen process molecules and enhances the immune response [68]. Fortunately, the sequence of the peptide presented Arg and Asp residues in the carboxyl-terminal sequence, and taking advantage of this situation, we inserted a Gly between these residues, resulting in the peptide 3 (p3) (KKFKPEIAIRPKVRGD). In summary, we obtained four candidate peptides as potential immunogenic agents: the original is predicted by PEPOP (KKFKPEIAIRPKVRDQEGRM) and its derivatives p1 (KKFKPEIAIRPKVRD), p2 (KLH-C-KKFKPEIAIRPKVRD), and p3 (KKFKPEIAIRPKVRGD).

Human IgG antibodies to the peptides

To elucidate the immunogenic and antigenic potential of the p1 and p2, an enzyme-linked immunosorbent assay (ELISA) was performed with sera of two volunteer groups. These groups were integrated by sera obtained from individuals who were considered prepandemic (i.e., sera samples obtained before 2009); these were in storage before the 2009 outbreak. The second group of sera was found to be pandemic because these samples were collected during the outbreak. This ELISA was based on the binding of human Ab (IgG) to the p1 and p2 (Figure 4) [69,70]. The IgG antibodies identified the p1 in the sera of the two groups with no significant statistical difference (analysis of variance (ANOVA)). These results show that the general population had antibodies against the p1 prior to the immunization or infection with other viruses or exposure to influenza A virus (H1N1). In other words, this epitope presumably is conserved among the pandemic and seasonal strains. Thus, the peptide is antigenic in humans. Results are presented as box-and-whisker plots. The boxes define the 25th and 75th percentiles, with error bars defining the 10th and 90th percentiles. Both peptides recognized human sera. Isotype response in serum from patients infected with influenza A p/H1N1/2009 IgG2 is the primary isotype of IgG antibodies against the p1. Although no differences were found in the levels of total IgG antibodies between prepandemic and pandemic sera, we analyzed the contribution of each subclass or isotype in response to p1 [71]. The antibody levels were significantly higher in the pandemic group compared with the prepandemic group (negative controls) for IgG2 ($P = 0.025$, Mann–Whitney U-test) and IgG4 subclasses ($P = 0.007$). In the rank order, IgG2 (0.6 vs. 0.5, median) > IgG4 (0.08 vs. 0.07, median). Peptide 1 is immunogenic and induced antibodies to the native form of HA. The rabbits immunized with p1 peptide and human infected with pH1N1 virus showed a definite immune response against wild-type viral antigens immobilized with concanavalin A (Con A, Sigma-Aldrich Corporation, St. Louis, MO, USA) (Figure 5). Rabbits immunized with p1 showed a stronger antibody response against the immobilized wild-type virus than human positive control. These results are significant and demonstrate that the p1 is highly immunogenic in rabbits and probably in humans, and it induces antibodies capable of interacting with the native form of HA [72].

Neutralizing antibodies induced by HA peptides in rabbits

Serum samples from rabbit immunized with p1 and from two vaccinated individuals and two patients infected with influenza A p/H1N1/2009 were titrated for neutralizing antibodies (PRNT50). p1 induces 1:533 neutralizing titers in rabbit, whereas the titers were 1:246 and 1:600 in vaccinated individuals and 1:400 and 1:250 in infected patients. On the other hand, p2, which is the p1 conjugated to hemocyanin (KLH-CKKFKPEIAIRPKVRD), and p3, in which a glycine was added between the arginine and the aspartate of the p1 sequence, induced neutralizing
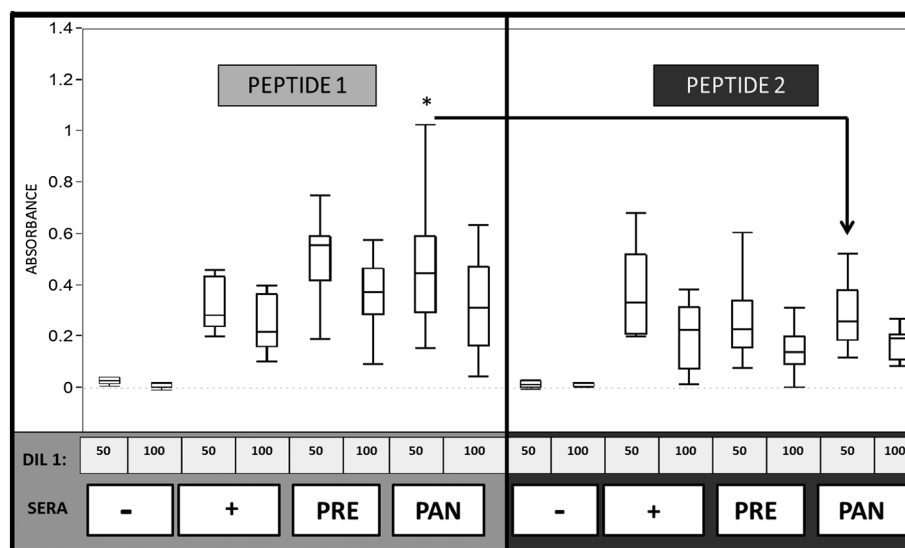

Figure 4. Detection of antibodies against P1 and P2. Microplates were coated with p1 or p2, and two dilutions (1:50 and 1:100) of sera from prepandemic and pandemic individuals were used. The IgG Ab to the HA peptide was detected with a secondary Ab specific for human IgG. *Statistical analysis of the ELISA, $p < 0.05$, Pandemic—p1 versus Pandemic—p2, dilution 1:50, one-way ANOVA, Tuckey–Kramer honestly significant difference.
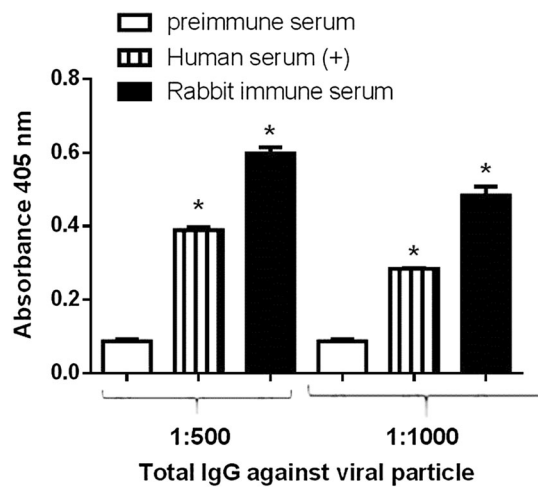
Figure 5. Levels of IgG against viral particle in serum of infected individuals or from rabbit immunized with peptide 1. IgG levels were determined by ELISA using viral antigens immobilized with Con A, and the IgG antibodies were detected with a secondary antibody specific for human or rabbit IgG. Data are expressed as the mean ± SD. The levels were significantly higher in human serum and rabbit antiserum ($p < 0.05$, Kruskal–Wallis).

antibodies in minor quantity in the infected or vaccinated group (titer 1: 103 and 1: 160, respectively) (Figure 6) [73,74].

DISCUSSION

Predicting of possible epitopes and testing their immunogenicity involve a full effort and intervention of diverse scientific disciplines. There are different epitope prediction methods based on biochemical properties, such as conserved sequences, special amino acids, length, hydrophobicity, secondary structure, and structure stability. Many studies focus on the sequence and its relation to B-cell immunity response; others take into account the recognition by MHC molecules or the 3D data of the proteins. Our workgroup has combined the epitope prediction and molecular modeling studies to obtain a peptide whose immunogenicity was assessed by experimental assays [70]. The area of opportunity for these studies is reflected by the fact that, until now, websites such as Immune Epitope Data Base (http://www.iedb.org/) that gather information on this topic are scarce [75,76]. In this work, we used the PEPOP epitope predictor because of its features and previous results. Later, we analyzed the localization of the epitope and its relationship with antigenic sites using the 3D model of HA (PDB ID: 3LZG). Once the sequence in 3D model of HA is localized, we identified that the epitope was located among the amino acids that conform to the Ca antigenic site and near Sa and Sb antigenic sites (Figure 1A and B). Interestingly, this finding initiates a discussion about the definition of continuous or discontinuous epitopes: if the sequence is not reported as a discontinuous epitope, at least, it is part of a continuous epitope. Thus, the ELISA could suggest that this sequence is part of the same antigenic site; more experimental assays are necessary to prove this asseveration [77–79]. To confirm the immunological capabilities of the epitopes initially predicted, these were submitted to other epitope predictors to select those that were found at least in three of these predictors (Figure 1C) [80,81]. Also, the conservation of the sequence should be considered in designing an epitope [82,83]. HA has different epitopes reported elsewhere; an example is the sequence IAI that is part of a peptide that produces efficient immune response for paracoccidioidomycosis granulomatous disease caused by *Paracoccidioides brasiliensis*, a thermal dimorphic fungus [84]. In the peptide reported in this work, the sequence IAI is between
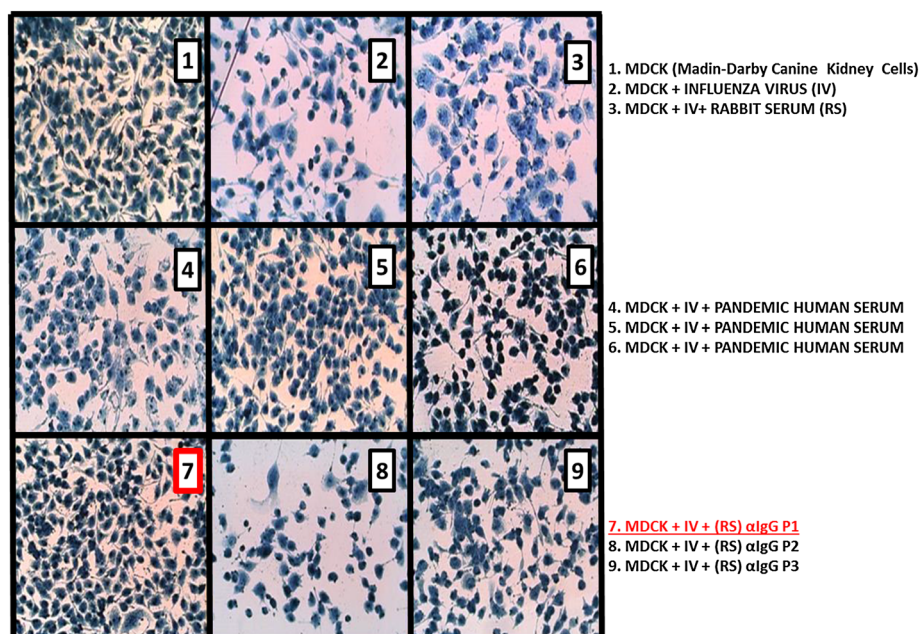

Figure 6. Plaque reduction neutralization test. Panel 1—MDCK cells, panel 2—MDCK cell with 30 plaque-forming units (PFU) influenza virus, panel 3—MDCK cells with Influenza virus and rabbit serum (not immunized). Panels 4–6—MDCK cell with 30 PFU and human sera, the three panels were controls. Panels 7–9—infected MDCK cells with immunized rabbit sera with peptides 1, 2, and 3.

residues 216 and 225 of the subunit 1 of the HA (3LZG). Rothbard and coworkers reported an extensive analysis of the DR1 epitopes, proposing different sequences and combinations of residues that could be recognized [85]. More recently, Yano and coworkers suggested the use of RGD sequence in vaccine design [86]. Our results showed that p3, with the sequence RGD, produces neutralizing antibodies, but it does not have the same reaction when compared with p1 in the neutralization assays, possibly because of the introduction of the Gly. Some of the structural changes have been studied by Dayan and coworkers, explaining the reason of this phenomenon [87]. Other authors have analyzed how the loss of the recognition is due to the flexibility of the interaction of MHC with peptide [88]. In the docking assay, we prepared the simulation to produce a high flexibility in the peptide and a rigid structure for the MHC molecule. However, the MD simulations allowed us to increase the relaxing of the epitope–MHC II complex in order to refine the 3D model of interaction. The structural analysis showed that the carboxy-terminal sequence maintains a rigid behavior, preventing an unfolding of the extreme of the peptide or the stretching out of the recognition groove. This conformation produced a strong turn that was maintained during the simulation between the P4 and P6, and it coincided with possible interaction with the Met20. The groove recognized three initial residues of the amino-terminal sequence; however, the size of the residues spanning from Lys12 to Ile17 of the peptide hinders the anchoring with the groove completely. Also, the two Arg residues of the peptide, the Asp and the Gln, could be a hindrance to an adequate docking given their hydrophobicity. Several authors have reported that the binding to the pocket P1 stabilizes the epitope–MHC II complex [89–91]. Herein, the computational simulations show that Lys1, Lys2, and Phe3 bind the hydrophobic pocket P1 and P4 (Figure 2). On the contrary, possibly, the presence of KHL interferes (hindrance effects) with the recognition by the antibodies. Lys1 and Lys2 could facilitate the antigen processing and the pocket anchoring. Further analyses are needed to explain this phenomenon. P4 was the most important anchoring element after the 100 ns of MD simulations, as is shown by the interactions with at least four residues of the peptide (Lys1, Lys2, Phe3, and Arg10). Mainly, the P4 of chain B plays the most important role. Thus, the RMSF analysis shows fewer fluctuations in the P4, which contains the residues of anchorage. Furthermore, P4 has been reported to elicit a suitable spatial disposition of the residues nearby. In turn, certain residues in P6 modify the conformation of those in P9. For instance, the binding of positively charged amino acids at P6 can reduce the cavity of P9, limiting the ability to interact with residues with hydrophobic side chains. In contrast, the binding of negatively charged amino acids at P6 enlarges P9, rendering P9 capable of accepting residues with large side chains. The strength of linear peptides to bind to each other is regularly associated with hydropathic complementarity. This occurs when peptides of different hydropathy bind to each other because hydrophilic amino acids in a peptide are located toward the aqueous solvent and release a space that could include a hydrophobic residue of the other peptide. The specificity of interactions between both peptides is improved by the ability of amino acids to create complementary protrusions and cavities and by the presence of residues of opposite charge [34]. According to MD simulations, the alpha helices of the recognition groove are unstable, particularly, in the alpha helices of both chains close to P1 and P4. Possibly, these changes are promoted by the interaction of the peptide (by Lys1, Lys2, and Phe3) with the lateral chains of MHC II, searching an appropriate interaction.

Peptide 1 manifested its immunogenicity by inducing antibodies in rabbits as shown in the neutralization assays. This property could be based on the molecular size, rigidity, chemical complexity, interaction with B-cell receptors, or MHC and activation of helper T cells [92]. The p1 proved to be an antigen that is recognized by the IgG Ab from immunized rabbits and infected individuals, using the methodology reported for other peptides [93–95]. IgG antibodies in human serum, mainly the IgG2 isotype, demonstrate that clinical or subclinical infections with the influenza virus induced IgG to the peptide. Thus, the peptide is immunogenic and antigenic in humans. Although we did not directly demonstrate the interaction of p1 with MHC II molecules in infected subjects, we believe that this interaction took place because class switching to produce IgG requires activated helper T cells that recognize the antigen (p1) in association with the MHC II protein on the surface of an antigen-presenting cell, such as B cells or dendritic cells. Moreover, the interaction of p1 with MHC II molecules and T helper cells (CD4 T cells) was demonstrated by the class switch of the IgG isotype, which is mediated by cytokines produced by T helper cell activation after recognition of the peptide on MHC II molecules and the engagement of the CD40 receptor on B cells by CD40 L [96–98]. Peptides are protected against proteolytic degradation because B cells contain much lower levels of lysosomal proteases than macrophages. This condition favors the presentation of antigenic peptides on MHC II molecules by limiting the complete destruction of the peptide determinants [99,100]. In addition, the B-cell receptor may protect the peptide from proteolytic enzymes (selective processing) [101]. Through these two mechanisms, p1 could interact with MHC II molecules as well as activated T helper cells and the production of IgG antibodies in humans and rabbits. To serve as an antigen, a molecule typically must have a relative molecular mass of at least 4000 Da, and the peptide under study is approximately 1.9 kDa (1825.21 Da, 15 amino acid residues). Interestingly, this p1 is one of the few substances with low molecular weight (below 2000) having immunogenic and antigenic properties [70]. Immunogenicity of a peptide is related to its amino acid composition and its diversity. As we mentioned earlier, Lys1, Lys2, and Phe3 contained in p1 interact with the pockets 1 and 4. In the native HA, the epitope corresponding to p1 is exposed, providing accessibility to Ab binding. Also, the polar residues are situated on the surface much more frequently than nonpolar residues; thus, the regions of highest average polarity within a polypeptide sequence have the highest likelihood of being targets for Ab binding. Evidence shows that mimic epitopes are continuous epitopes, specifically the sera from all the individual of our trial recognized the peptide p1. Therefore, we confirmed that is a B-cell epitope, and it has been circulated previously in Mexican population, where clinical or subclinical infections with the influenza virus induced IgG Ab to the peptide p1. The antibodies against p1 were mainly isotype IgG2, which is the most abundant in human sera. IgG2 isotype is less efficient for complement activation and antibody dependent cell-mediated cytotoxicity than other isotypes, such as IgG1 [102,103]. We propose that the effect of IgG2 isotype against peptide 1 could be the neutralization of the free virus, producing antiviral activity through the binding of antibodies to the receptor binding site of the HA and preventing the infection by the influenza virus [42]. Moreover, the protection with IgG2 is

noteworthy because patients with a severe infection with influenza H1N1 have lower levels of this isotype and p1 peptide induces this isotype. Nevertheless, it is necessary to determine the neutralizing activity of the IgG2 isotype [104]. Finally, the results of the Con A and PRNT assays demonstrate that the peptides induce antibodies that can react with the protein of wild-type virus and neutralize it. The titers in vaccinated individuals were 1:246 and 1:600 and in infected patients were 1:400 and 1:250. These results suggest that the p1 induce a reaction similar to vaccine or in infected patients with titers of 1:533 and might be a candidate to be used as a peptide-based vaccine or in a diagnosis tool of the human influenza AH1N1.

MATERIAL AND METHODS

Ethics statement

The protocols for rabbits were reviewed and approved by the Committee of Bioethics and Research of the Escuela Nacional de Medicina y Homeopatía del IPN, Mexico City. The animals were handled in accordance with the Mexican Official Regulation (NOM-062-Z00-199—technical specifications for production, care, and use of laboratory animals). All serum samples for experiments were obtained from donors after they signed a written informed consent according to the Declaration of Helsinki.

Epitope prediction

The crystal structure used for this study was the HA reported by Xu and coworkers (PDB code: 3LZG) [42]. All predictions were performed with the sequence and structure of 3LZG. Six programs of epitope predictions, four sequential predictors, and two structural predictors were used. To obtain MHC II epitope predictions, PROPED2 was utilized (http://www.imtech.res.in/raghava/propred/); its predictions are based on locating the promiscuous regions that can bind HLA-DR alleles [28], including the 47 HLA-DRB1s, which are the most representative. The MHC2PRED program (http://www.imtech.res.in/raghava/mhc2pred/info.html) was also used to obtain MHC II epitope predictions. Each peptide is represented by a 20-dimensional vector (SMV) using 12 alleles of its matrix (10 HLA-DRB1, 1 HLA-DRB5, and 1 HLA-DRB4) [26]. NetCTL 1.2 server predicts CTL epitopes in protein sequences that expand the MHC class I binding prediction to 12 MHC supertypes [105]. Finally, the last sequential predictor used was Vaxign [106] that is a vaccine target prediction and analysis system based on the principle of reverse vaccinology. Using 3D coordinates of the two chains of the model, we submit to both structural predictors, PEPOP (http://pepop.sysdiag.cnrs.fr/PEPOP/) [24] and SEPPA (http://lifecenter.sgst.cn/seppa/) [107]. We used the coordinates of the two chains of the model and submitted them to both predictors (Figure S1).

Docking the epitope with the MHC II

Once the best epitope was obtained, a docking study was employed to describe the epitope and MHC II interactions. The crystal structure of MHC II for this analysis was HLA-DRB1*0401 (PDB ID: 1D5M). HLA-DRB1 was previously reported to predict response profiles in donors when HLA haplotypes in the H1N1 virus were chosen at random [108]. Importantly, this HLA-DR allele is present in the majority of the human population [109].

We performed a non-restricted docking with the CLUSPRO automated docking program [54]. Docking calculations were also performed with AutoDock 4.0.1 [110]. The search space was restricted to a rectangular box that included β-folded chains and α-helix chains targeting the binding site of the epitope and the MHC II. A rectangular grid ($70 \times 100 \times 90$ Å) with points separated by 0.375 Å was generated. The docking parameters of 100 runs with 100 million energy evaluations for each test and a population size of 100 individuals were used. The docking results were analyzed with AutoDock Tools and PyMol software [53].

Molecular dynamics simulation

The software GROMACS performed the MD simulations. First, the system was embedded in a solvated water box, and then the system was neutralized. The system had undergone an equilibration process before MD simulations were performed. The equilibration started with an initial minimization and was followed by whole minimization. Then an MD simulation of water molecules was carried out with all backbone atoms fixed. Finally, a 100-ns MD simulation was achieved under ensemble number of particles, system volume, and temperature (NVT). Tools of GROMACS were used to calculate the RMSD and RMSF [111].

Contact map

To analyze the contacts and distances of the complex, a program of the Weizmann Institute of Science in Israel (http://ligin.weizmann.ac.il/cma) was performed to generate the contact map.

Peptide synthesis

Three peptides were purchased for immunological assays as crude material from Mimotopes (Minneapolis, MN, USA and Clayton, Victoria, Australia): peptide 1 (p1: KKFKPEIAIRPKVRD), peptide 2 (p2: KLH-CKKFKPEIAIRPKVRD) conjugated with hemocyanin (KLH) linked to a cysteine with the sequence of the p1, and peptide 3 (p3: KKFKPEIAIRPKVRGD) with the addition of a glycine between the arginine and the aspartate.

Enzyme-linked immunosorbent assay

Blood was obtained according to previously reported procedures [70] from healthy individuals who were living in Mexico City before the outbreak of the influenza H1N1 virus in 2009 and volunteers after the peak of the pandemic. Anti-HA peptide levels were evaluated in serum samples from infected and asymptomatic persons. The Ab levels in the serum samples were quantified by an indirect ELISA; 96-well plates were coated with either p1 or p2. One microgram per milliliter of peptide in carbonate bicarbonate buffer (15 mM Na_2CO_3 and 35 mM $NaHCO_3$ at pH 9.6) was used. The plates were incubated for 2 h at 37 °C and washed three times with 0.05% Tween-20 in phosphate-buffered saline (PBST). Blocking was performed by treating with PBST plus 6% fat-free milk and by further washing with PBST. Each sample was tested in duplicate. Serum samples from individuals were diluted 1:50 or 1:100. Afterward, the plates were incubated overnight at 4 °C and washed with PBST. Dilutions of 1:1000, 1:2000, and 1:4000 goat anti-mouse IgG (Santa Cruz Biotechnology) or rabbit anti-human IgG (1:1000, Santa Cruz Biotechnology) were added to each well, and the plates were incubated for 2 h at room temperature. The plates were washed

with PBST, and the enzymatic reactions were begun by adding substrate solution (0.5 mg/mL o-phenylenediamine plus 0.01% H_2O_2 in 0.05 M citrate buffer 291 at pH 5.2). After 15 min, the reactions were stopped with 25 μL of 2.5 M H_2SO_4, and the absorbance at 492 nm (A 492) was measured using a Multiscan Ascent (Thermo Labsystems Inc., Philadelphia, PA, USA) microplate reader [112].

Immunization of rabbits

Three rabbits were immunized with the three designed peptides (p1, p2, and p3). The immunization schedule was as follows. On day 1 (first immunization), 300 μg of peptide plus complete Freund's adjuvant (Sigma Chemical Co., St. Louis, MO, USA) was administered through the subcutaneous route. On day 8 (second immunization), 300 μg of peptide plus incomplete Freund's adjuvant was administered through the subcutaneous route. On day 15 (third immunization), 300 μg of peptide in 5 mL of saline solution was supplied via intramuscular injection. Seven days after the last immunization, the rabbits were anesthetized with pentobarbital, and serum samples were obtained from blood extracted by cardiac puncture and stored at −70 °C [70].

Cells and influenza viruses

Madin-Darby canine kidney (MDCK) cells were grown in Dulbecco's Modified Eagle Medium Nutrient Mixture F-12 (DMEM/F-12) (Gibco, Grand Island, NY, USA), supplemented with 10% fetal bovine serum (Invitrogen) at 37 °C and 5% CO_2. The strain influenza A Puerto Rico/916/34 (PubMed identifier: 24146939) was gently donated by Dr. Blanca Lilia Barrón, and the stock was prepared and stored as previously described [113].

Concanavalin A enzyme-linked immunosorbent assay

Viral particles isolated and purified (FBS free) from infected MDCK cells were immobilized in wells coated with Con A, which binds the glycoproteins of enveloped viruses. Briefly, 96-well plates (Costar) were coated with 100 μL per well of Con A at 50 μg/mL in PBS, pH 7.4 for 1 h. The wells were washed and incubated with solubilized influenza A Puerto Rico/916/34 (serum-free virus stock) in PBS containing 0.1% Triton-X (PBS-Tx) for 1 h. After the wells had been washed with PBS-Tx, the unbound Con A binding sites were blocked with Roswell Park Memorial Institute medium 1640 containing 10% FBS for 1 h. Serial dilutions of the serum samples were incubated for 1 h at room temperature. Serum from influenza-positive patients was used as a positive control. Rabbit pre-immune serum samples were used as negative controls. After the wells had been washed again, they were incubated with 100 μL of peroxidase-conjugated secondary antibody anti-IgG (H + L) (Invitrogen) [72].

Neutralization assay

Neutralizing antibodies were titrated as described previously by Morens and coworkers. Briefly, serial dilutions of the heat-inactivated test sera in triplicate started from 1:20 were mixed with 20 plaque-forming units of influenza A Puerto Rico/916/34 virus for 1 h at 37 °C and added to MDCK at a density of 1.2×10^5 Use 120,000 cells per well in 24-well plates. At 1 h after infection, serum-free DMEM/F-12 medium with 2 μg of L-1-tosylamide-2-phenyl ethyl chloromethyl ketone-treated trypsin was added to each well for 10 min at 37 °C. Then 500 μL of overlay medium

was added to each well, and plates were incubated for 3 days under the same conditions. The supernatant was discarded, and the plaques were visualized with naphthol blue-black dye. The cytopathic effect was evaluated to determine the highest serum dilution that protected 50% of the cells from cytopathology in these wells. Positive and negative control sera and virus back titration were included in the assay to confirm the viral inoculum [73,74].

Isotype response in serum from patients infected with pandemic influenza AH1N1 2009

IgG isotype antibodies against p1 peptide were measured by ELISA in 96-well polyvinyl plates (Nunc) coated with each peptide (2 μg/mL). We assayed 40 sera from patients infected with influenza AH1N1 2009 and 40 prepandemic sera at 1:100 dilutions for 1 h at 37 °C. Then the anti-human immunoglobulin peroxidase-conjugated secondary antibodies were added (anti-human IgG1, 2, 3, or 4, all Invitrogen) for 1 h at 37 °C. After H_2O_2 and 2,2′-azino-bis(3-ethylbenzothiazoline-6-sulfonic acid) (Sigma-Aldrich Corporation, St. Louis, MO, USA) were added as substrates. The absorbance values were determined at 405 nm [71].

Statistical analysis

Statistical analyses were performed using JMP Statistical Software (SAS Institute, Cary, NC, USA) (http://www.jmp.com/). Normally distributed data were analyzed by one-way ANOVA test to compare the groups. The differences among the groups were analyzed by a Tukey–Kramer honestly significant difference test; differences were considered significant at $p < 0.05$. Isotype differences were analyzed by ANOVA and Mann–Whitney U-test, t-test, nonparametric test, and Mann–Whitney post-test using GraphPad Prism 6 program (GraphPad Software, Inc., CA, USA) to determine the significance of the differences between groups, denoted by asterisks as follows: $*p < 0.05$, $**p < 0.01$.

CONCLUSION

In addition to offering an atomistic description of the interaction of a peptide with the MHC, this study showed that *in silico* experiments (prediction of immunogenic epitopes, docking, and MD simulation) are useful tools for the rational design of epitope vaccines. An example is offered in this work using the HA protein of the influenza AH1N1 virus, whose resultant peptide can be used as a diagnostic tool or as an immunogenic agent. This strategy includes an experimental evaluation of immunogenic epitopes and could decrease the economic investment and the time needed to obtain epitope vaccines and diagnostic tools. Our research indicates that the selected peptide is immunogenic, antigenic, and efficient in inducing a strong immune response. Therefore, it should be a good candidate for the development of a peptide-based vaccine or diagnostic tool.

REFERENCES

1. Meltzer MI, Cox NJ, Fukuda K 1999. The economic impact of pandemic influenza in the United States: priorities for intervention. *Emerg Infect Dis* **5**: 659–671. DOI: 10.3201/eid0505.990507.

2. Eccles R 2005. Understanding the symptoms of the common cold and influenza. *Lancet Infect Dis* **5**: 718–725. DOI: 10.1016/S1473-3099(05)70270-X.

3. Simonsen L, Matthew JC, Lawrence BS, Nancy HA, Nancy JC, Keiji F 1998. Pandemic versus epidemic influenza mortality: a pattern of changing age distribution. *J Infect Dis* **178**: 53–60. DOI: 10.1086/515616.

4. Steinhauer DA, Skehel JJ. 2002. Genetics of influenza viruses. *Annu Rev Genet* **36**: 305–332. DOI: 10.1146/annurev.genet.36.052402.152757.

5. Wood JM. 2001. Developing vaccines against pandemic influenza. *Philos Trans R Soc Lond B Biol Sci* **29**: 1953–1960. DOI: 10.1098/rstb.2001.0981.

6. Kaiser J. 2006. A one-size-fits-all flu vaccine? *Science* **5772**: 380–382. DOI: 10.1126/science.312.5772.380.

7. Lu Y, Ding J, Liu W, Chen YH. 2002. A candidate vaccine against influenza virus intensively improved the immunogenicity of a neutralizing epitope. *Int Arch Allergy Immunol* **127**: 245–250. DOI: 10.1159/000053869.

8. Plotkin JB, Dushoff J. 2003. Codon bias and frequency-dependent selection on the hemagglutinin epitopes of influenza A virus. *Proc Natl Acad Sci U S A* **100**: 127152–127157. DOI: 10.1073/pnas.1132114100.

9. Ekiert DC, Bhabha G, Elsliger MA, Friesen RH, Jongeneelen M, Throsby M, Goudsmit J, Wilson IA. 2009. Antibody recognition of a highly conserved influenza virus epitope. *Science* **324**: 246–251. DOI: 10.1126/science.1171491.

10. Novotný J, Handschumacher M, Haber E, Bruccoleri RE, Carlson WB, Fanning DW, Smith JA, Rose GD. 1986 Antigenic determinants in proteins coincide with surface regions accessible to large probes (antibody domains). *Proc Natl Acad Sci U S A* **83**: 226–230.

11. Liu W, Peng Z, Liu Z, Lu Y, Ding J, Chen YH. 2004. High epitope density in a single recombinant protein molecule of the extracellular domain of influenza A virus M2 protein significantly enhances protective immunity. *Vaccine* **23**: 366–371.DOI: 10.1016/j.vaccine.2004.05.028.

12. Zou P, Liu W, Chen YH. 2005. The epitope recognized by a monoclonal antibody in influenza A virus M2 protein is immunogenic and confers immune protection. *Int Immunopharmacol* **5**: 631–635. DOI: 10.1016/j.intimp. 2004.12.005.

13. Garten RJ, Davis CT, Russell CA, Shu B, Lindstrom S, Balish A, Sessions WM, Xu X, Skepner E, Deyde V, Okomo-Adhiambo M, Gubareva L, Barnes J, Smith CB, Emery SL, Hillman MJ, Rivailler P, Smagala J, de Graaf M, Burke DF, Fouchier RAM, Pappas C, Alpuche-Aranda CM, López-Gatell H, Olivera H, López I, Myers CA, Faix D, Blair PJ, Yu C, Keene KM, Dotson PD, Jr., Boxrud D, Sambol AR, Abid SH, St. George K, Bannerman T, Moore AL, Stringer DJ, Blevins P, Demmler-Harrison GJ, Ginsberg M, Kriner P, Waterman S, Smole S, Guevara HF, Belongia EA, Clark PA, Beatrice ST, Donis R, Katz J, Finelli L, Bridges CB, Shaw M, Jernigan DB, Uyeki TM, Smith DJ, Klimov AI, Cox NJ. 2009. Antigenic and genetic characteristics of swine-origin 2009 A(H1N1) influenza viruses circulating in humans. *Science* **325**: 197–201. DOI: 10.1126/science.1176225.

14. Goh GK, Dunker AK, Uversky VN. 2009. Protein intrinsic disorder and influenza virulence: the 1918 H1N1 and H5N1 viruses. *Virol J* **6**: 69. DOI: 10.1186/1743-422X-6-69.

15. Heiny AT, Miotto O, Srinivasan KN, Khan AM, Zhang GL, Brusic V, Tan TW, August JT. 2007. Evolutionarily conserved protein sequences of influenza a viruses, avian and human, as vaccine targets. *PLoS One* **2**(11): e1190. DOI: 10.1371/journal.pone.0001190.

16. Shih AC, Hsiao TC, Ho MS, Li WH. 2007. Simultaneous amino acid substitutions at antigenic sites drive influenza A hemagglutinin evolution. *Proc Natl Acad Sci U S A* **104**: 6283–6288. DOI: 10.1073/pnas.0701396104.

17. Gogolák P, Simon A, Horváth A, Réthi B, Simon I, Berkics K, Rajnavölgyi E, Tóth GK. 2000. Mapping of a protective helper T cell epitope of human influenza A virus hemagglutinin. *Biochem Biophys Res Commun* **270**: 190–198. DOI: 10.1006/bbrc.2000.2384.

18. Caton AJ, Brownlee GG, Yewdell JW & Gerhard W. 1982. The antigenic structure of the influenza virus A/PR/8/34 hemagglutinin (H1 subtype). *Cell* **31**: 417–427. DOI: 10.1016/0092-8674(82)90135–0.

19. Wilson DB, Pinilla C, Wilson DH, Schroder K, Boggiano C, Judkowski V, Kaye J, Hemmer B, Martin R, Houghten RA. 1999. Immunogenicity. I. Use of peptide libraries to identify epitopes that activate clonotypic CD4+ T cells and induce T cell responses to native peptide ligands. *J Immunol* **163**: 6424–6434.

20. Seyed N, Zahedifard F, Safaiyan S, Gholami E, Doustdari F, Azadmanesh K, Mirzaei M, Saeedi Eslami N, Khadem Sadegh A, Eslami Far A, Sharifi I, Rafati S. 2011. In silico analysis of six known *Leishmania major* antigens and in vitro evaluation of specific epitopes eliciting HLA-A2 restricted CD8 T cell response. *PLoS Negl Trop Dis* **5**(9): e1295. DOI: 10.1371/journal.pntd.0001295.

21. Wang LF, Yu M. 2004. Epitope identification and discovery using phage display libraries: applications in vaccine development and diagnostics. *Curr Drug Targets* **5**: 1–15. DOI: 10.2174/1389450043490668.

22. Schwaiger J, Aberle JH, Stiasny K, Knapp B, Schreiner W, Fae I, Fischer G, Scheinost O, Chmelik V, Heinz FX. 2014. Specificities of human CD4+ T cell responses to an inactivated Flavivirus vaccine and infection: correlation with structure and epitope prediction. *J Virol* **88**: 7828–7842. DOI: 10.1128/JVI.00196-14.

23. Chen P, Rayner S, Hu KH. 2011. Advances of bioinformatics tools applied in virus epitopes prediction. *Virol Sin* **26**: 1–7. DOI: 10.1007/s12250-011-3159-4.

24. Moreau V, Fleury C, Piquer D, Nguyen C, Novali N, Villard S, Laune D, Granier C, Molina F. 2008. PEPOP: computational design of immunogenic peptides. *BMC Bioinf* **9**: 71. DOI: 10.1186/1471-2105-9-71.

25. Wu D, Xu TL, Sun J, Dai JX, Ding GH, He Y, Zhou ZF, Xiong H, Dong H, Jin WR, Bian C, Jin L, Wang HY, Wang XN, Yang Z, Zhong Y, Wang H, Che XY, Huang Z, Lan K, Sun B, Wu F, Yuan ZA, Zhang X, Zhou XN, Zhou JH, Ma ZY, Tong GZ, Guo YJ, Zhao GP, Li YX, Cao ZW. 2009. Structure modeling and spatial epitope analysis for HA protein of the novel H1N1 influenza virus. *Chin Sci Bull* **54**: 2171–2173. DOI: 10.1007/s11434-009-0429-3.

26. Wang L, Pan D, Hu X, Xiao J, Gao Y, Zhang H, Zhang Y, Liu J, Zhu S. 2009. BiodMHC: an online server for the prediction of MHC class II-peptide binding affinity. *J Genet Genomics* **36**: 289–296. DOI: 10.1016/S1673-8527(08)60117-4.

27. Lata S, Bhasin M, Raghava GP. 2007. Application of machine learning techniques in predicting MHC binders. *Methods Mol Biol* **409**: 201–215. DOI: 10.1007/978-1-60327-118-9_14

28. Singh H, Raghava GP. 2001. ProPred: prediction of HLA-DR binding sites. *Bioinformatics* **17**: 1236–1237. doi: 10.1093/bioinformatics/17.12.1236.

29. Malito E, Rappuoli R. 2013. Finding epitopes with computers. *Chem Biol* **20**: 1205–1206. DOI: 10.1016/j.chembiol.2013.10.002.

30. Zoete V, Irving M, Ferber M, Cuendet MA, Michielin O. 2013. Structure-based, rational design of T cell receptors. *Front Immunol* **4**: 268. DOI: 10.3389/fimmu.2013.00268.

31. Sela-Culang I, Benhnia MR, Matho MH, Kaever T, Maybeno M, Schlossman A, Nimrod G, Li S, Xiang Y, Zajonc D, Crotty S, Ofran Y, Peters B. 2014. Using a combined computational-experimental approach to predict antibody-specific B cell epitopes. *Structure* **22**: 646–657. DOI: 10.1016/j.str.2014.02.003.

32. Hoze E, Tsaban L, Maman Y, Louzoun Y. 2013. Predictor for the effect of amino acid composition on CD4+ T cell epitopes preprocessing. *J Immunol Methods* **391**: 163–173. DOI: 10.1016/j.jim.2013.02.006.

33. Van Regenmortel MH (2009) Synthetic peptide vaccines and the search for neutralization B cell epitopes *The Open Vaccine Journal* **2**: 33–44.

34. Van Regenmortel MH. 2014. Specificity, polyspecificity, and heterospecificity of antibody–antigen recognition *J Mol Recognit* **27**: 627–639. DOI: 10.1002/jmr.2394.

35. Flower DR, Macdonald IK, Ramakrishnan K, Davies MN, Doytchinova IA. 2010. Computer aided selection of candidate vaccine antigens. *Immunome Res* **6**: S1. DOI: 10.1186/1745-7580-6-S2–S.

36. Chen J, Wang Y, Guo D, Shen B. 2012. A systems biology perspective on rational design of peptide vaccine against virus infections. *Curr Top Med Chem* **12**: 1310–1319 DOI: 10.2174/156802612801319043.

37. Ponomarenko JV & Bourne PE. 2007. Antibody–protein interactions: benchmark datasets and prediction tools evaluation. *BMC Struct Biol* **7**: 64. DOI: 10.1186/1472-6807-7-64.

38. Krawczyk K, Liu X, Baker T, Shi J, Deane CM. 2014. Improving B-cell epitope prediction and its application to global antibody-antigen docking. *Bioinformatics* DOI: 10.1093/bioinformatics/btu190.

39. Knapp B, Omasits U, Schreiner W, Epstein MM. 2010. A comparative approach linking molecular dynamics of altered peptide ligands

and MHC with in vivo immune responses. *PLoS One* **5**(7): e11653. DOI: 10.1371/journal.pone.0011653.

40. Stavrakoudis A. 2010. Conformational flexibility in designing peptides for immunology: the molecular dynamics approach. *Curr Comput Aided Drug Des* **6**: 207–222. DOI: 10.2174/157340910791760073.

41. Somvanshi P, Singh V, Seth PK. 2008. Prediction of epitopes in hemagglutinin and neuraminidase proteins of influenza A virus H5N1 strain: a clue for diagnostic and vaccine development. *OMICS* **12**: 61–69. DOI: 10.1089/omi.2007.0037.

42. Xu R, Ekiert DC, Krause JC, Hai R, Crowe JE Jr, Wilson IA. 2010. Structural basis of preexisting immunity to the 2009 H1N1 pandemic influenza virus. *Science* **328**: 357–360. DOI: 10.1126/science.1186430.

43. Jørgensen KW, Buus S, Nielsen M. 2010. Structural properties of MHC class II ligands, implications for the prediction of MHC class II epitopes. *PLoS One* **5**(12): e15877. DOI: 10.1371/journal.pone.0015877.

44. Sinigaglia F, Hammer J. 1994. Rules for peptide binding to MHC class II molecules. *APMIS* **102**: 241–248. DOI: 10.1111/j.1699-0463.1994.tb04871.x.

45. Madden DR, Garboczi DN, Wiley DC. 1993. The antigenic identity of peptide–MHC complexes: a comparison of the conformations of five viral peptides presented by HLA-A2. *Cell* **75**: 693–708 DOI: 10.1016/0092-8674(93)90490-H.

46. Trombetta ES, Mellman I. 2005. Cell biology of antigen processing in vitro and in vivo. *Annu Rev Immunol* **23**: 975–1028. DOI: 10.1146/annurev.immunol.22.012703.104538.

47. Villadangos JA. 2001. Presentation of antigens by MHC class II molecules: getting the most out of them. *Mol Immunol* **38**: 329–346. DOI: 10.1016/S0161-5890(01)00069-4.

48. Wiley DC, Skehel JJ. 1987. The structure and function of the hemagglutinin membrane glycoprotein of influenza virus. *Annu Rev Plant Physiol Plant Mol Biol* **56**: 365–394 DOI: 10.1146/annurev.bi.56.070187.002053.

49. Meroz D, Yoon SW, Ducatez MF, Fabrizio TP, Webby RJ, Hertz T Ben-Tal N. 2011. Putative amino acid determinants of the emergence of the 2009 influenza A (H1N1) virus in the human population. *Proc Natl Acad Sci U S A* **108**: 13522–13527. DOI: 10.1073/pnas.1014854108.

50. Ménez R, Bossus M, Muller BH, Sibaï G, Dalbon P, Ducancel F, Jolivet-Reynaud C, Stura EA. 2003. Crystal structure of a hydrophobic immunodominant antigenic site on hepatitis C virus core protein complexed to monoclonal antibody 19D9D6. *J Immunol* **170**: 1917–1924.

51. Kropshofer H, Max H, Müller CA, Hesse F, Stevanovic S, Jung G, Kalbacher H. 1992. Self-peptide released from class II HLA-DR1 exhibits a hydrophobic two-residue contact motif. *J Exp Med* **175**: 1799–1803. DOI: 10.1084/jem.175.6.1799.

52. Walavalkar NM, Gordon N, Williams DC Jr.. 2013. Unique features of the antiparallel, heterodimeric coiled-coil interaction between methyl-cytosine binding domain 2 (MBD2) homologues and GATA zinc finger domain containing 2A (GATAD2A/p66α) *J Biol Chem* **288**: 3419–3427 DOI: 10.1074/jbc.M112.431346.

53. Seeliger D, de Groot BL. 2010. Ligand docking and binding site analysis with PyMOL and AutoDock/Vina. *J Comput Aided Mol Des* **24**: 417–422. DOI: 10.1007/s10822- 010-9352-6.

54. Comeau SR, Gatchell DW, Vajda S, Camacho CJ. 2004. ClusPro: an automated docking and discrimination method for the prediction of protein complexes. *Bioinformatics* **20**: 45–50. DOI: 10.1093/bioinformatics/btg371.

55. Amaro RE, Baron R, McCammon JA. 2008. An improved relaxed complex scheme for receptor flexibility in computer-aided drug design. *J Comput Aided Mol Des* **22**: 693–705. DOI: 10.1007/s10822-007-9159-2.

56. Terentiev AA, Moldogazieva NT, Levtsova OV, Maximenko DM, Borozdenko DA, Shaitan KV. 2012. Modeling of three dimensional structure of human alpha-fetoprotein complexed with diethylstilbestrol: docking and molecular dynamics simulation study *J Bioinform Comput Biol* **10**: 1241012. DOI: 10.1142/S0219720012410120.

57. Carlsson J, Boukharta L, Aqvist J (2008) Combining docking, molecular dynamics and the linear interaction energy method to predict binding modes and affinities for nonnucleoside inhibitors to HIV-1 reverse transcriptase. *J Med Chem* **51**: 2648–2656. DOI: 10.1021/jm7012198.

58. Shahlaei M, Madadkar-Sobhani A, Mahnam K, Fassihi A, Saghaie L & Mansourian M. 2011. Homology modeling of human CCR5 and analysis of its binding properties through molecular docking and molecular dynamics simulation. *Biochim Biophys Acta* **1808**: 802–817. DOI: 10.1016/j.bbamem.2010.12.004.

59. Król M, Chaleil RA, Tournier AL, Bates PA. 2007. Implicit flexibility in protein docking: cross-docking and local refinement. *Proteins* **69**: 750–757. DOI: 10.1002/prot.2169.

60. Senda Y, Fujio M, Shimamura S, Blomqvist J, Nieminen RM. 2012. Fast convergence to equilibrium for long-chain polymer melts using a MD/continuum hybrid method. *J Chem Phys* **137**: 154115. DOI: 10.1063/1.4759036.

61. Grossfield A, Feller SE, Pitman MC. 2007. Convergence of molecular dynamics simulations of membrane proteins. *Proteins* **67**: 31–40. DOI: 10.1002/prot.21308.

62. Smith LJ, Daura X, Van Gunsteren WF. 2002. Assessing equilibration and convergence in biomolecular simulations. *Proteins* **48**: 487–496. DOI: 10.1002/prot.10144.

63. Sundaram R, Lynch MP, Rawale SV, Sun Y, Kazanji M, Kaumaya PT. 2004. De novo design of peptide immunogens that mimic the coiled coil region of human T-cell leukemia virus type-1 glycoprotein 21 transmembrane subunit for induction of native protein reactive neutralizing antibodies. *Biol Chem* **279**: 24141–24151 DOI: 10.1074/jbc.M313210200.

64. Kaumaya PT, VanBuskirk AM, Goldberg E, Pierce SK. 1992. Design and immunological properties of topographic immunogenic determinants of a protein antigen (LDH-C4) as vaccines. *J Biol Chem* **267**: 6338–6346.

65. Wang CY, Chang TY, Walfield AM, Ye J, Shen M, Ye J, Chen SP, Li MC, Lin YL, Jong MH, Yang PC, Chyr N, Kramer E, Brown F. 2002. Effective synthetic peptide vaccine for foot-and-mouth disease in swine. *Vaccine* **20**: 2603–2610. DOI: 10.1016/S0264-410X(02)00148-2.

66. Yano A, Onozuka A, Asahi-Ozaki Y, Imai S, Hanada N, Miwa Y, Nisizawa T (2005) An ingenious design for peptide vaccines. *Vaccine* **23**: 2322–2326. DOI: 10.1016/j.vaccine.2005.01.031.

67. Helling F, Shang A, Calves M, Zhang S, Ren S, Yu RK, Oettgen HF, Livingston PO. 1994. GD3 vaccines for melanoma: superior immunogenicity of keyhole limpet hemocyanin conjugate vaccines. *Cancer Res* **54**: 197–203.

68. Yano A, Onozuka A, Matin K, Imai S, Hanada N, Nisizawa T. 2003. RGD motif enhances immunogenicity and adjuvanicity of peptide antigens following intranasal immunization. *Vaccine* **22**: 237–243. DOI: 10.1016/S0264-410X(03)00561-9.

69. Mavrouli MD, Routsias JG, Maltezou HC, Spanakis N, Tsakris A. 2011. Estimation of seroprevalence of the pandemic H1N1 2009 influenza virus using a novel virus-free ELISA assay for the detection of specific antibodies. *Viral Immunol* **24**: 221–226. DOI: 10.1089/vim.2010.0137.

70. Loyola PK, Campos-Rodríguez R, Bello M, Rojas-Hernández S, Zimic M, Quiliano, M, Briz V, Muñoz-Fernández MA, Tolentino-López L, Correa-Basurto J. 2013. Theoretical analysis of the neuraminidase epitope of the Mexican A H1N1 influenza strain, and experimental studies on its interaction with rabbit and human hosts. *Immunol Res* **56**: 44–60. DOI: 10.1007/s12026-013-8385-z.

71. Burlington DB, Clements ML, Meiklejohn G, Phelan M, Murphy BR. 1983. Hemagglutinin-specific antibody responses in immunoglobulin G, A, and M isotypes as measured by enzyme-linked immunosorbent assay after primary or secondary infection of humans with influenza A virus. *Infect Immun* **41**: 540–545.

72. Robinson JE, Holton D, Liu J, McMurdo H, Murciano A, Gohd R. 1990. A novel enzyme-linked immunosorbent assay (ELISA) for the detection of antibodies to HIV-1 envelope glycoproteins based on immobilization of viral glycoproteins in microtiter wells coated with concanavalin A. *J Immunol Methods* **132**: 63–71. DOI: 10.1016/0022-1759(90)90399-G.

73. Chan KH, To KK, Hung IF, Zhang AJ, Chan JF, Cheng VC, Tse H, Che XY, Chen H, Yuen KY. 2011. Differences in antibody responses of individuals with natural infection and those vaccinated against pandemic H1N1 2009 influenza. *Clin Vaccine Immunol* **18**: 867–873. DOI: 10.1128/CVI.00555-10.

74. Morens DM, Halstead SB, Repik PM, Putvatana R, Raybourne N. 1985. Simplified plaque reduction neutralization assay for dengue viruses by semimicromethods in BHK-21 cells: comparison of the BHK suspension test with standard plaque reduction neutralization. *J Clin Microbiol* **22**: 250–254.

75. Geysen HM, Barteling SJ, Meloen RH. 1985. Small peptides induce antibodies with a sequence and structural requirement for binding antigen comparable to antibodies raised against the native protein. *Proc Natl Acad Sci U S A* **82**: 178–182. doi:10.1073/pnas.82.1.178.

76. Peters B, Sidney J, Bourne P, Bui HH, Buus S, Doh G, Fleri W, Kronenberg M, Kubo R, Lund O, Nemazee D, Ponomarenko JV,

Sathiamurthy M, Schoenberger S, Stewart S, Surko P, Way S, Wilson S, Sette A. 2005. The immune epitope database and analysis resource: from vision to blueprint. *PLoS Biol* **3**(3): e91.DOI: 10.1371/journal.pbio.0030091.

77. Wiegers KJ, Wetz K, Dernick R. 1990. Molecular basis for linkage of a continuous and discontinuous neutralization epitope on the structural polypeptide VP2 of poliovirus type 1. *J Virol* **64**: 1283–1289.

78. Moreau V, Granier C, Villard S, Laune D, Molina F. 2006. Discontinuous epitope prediction based on mimotope analysis. *Bioinformatics* **22**: 1088–1095. DOI: 10.1093/bioinformatics/btl012.

79. Flower DR. 2003. Towards in silico prediction of immunogenic epitopes. *Trends Immunol* **24**(12): 667–674. DOI: 10.1016/j.it.2003.10.006.

80. Yu K, Petrovsky N, Schönbach C, Koh JY, Brusic V. 2002. Methods for prediction of peptide binding to MHC molecules: a comparative study. *Mol Med* **8**: 137–148.

81. Igarashi M, Ito K, Yoshida R, Tomabechi D, Kida H, *et al.*, 2010. Predicting the antigenic structure of the pandemic (H1N1) 2009 influenza virus hemagglutinin. *PLoS One* **5**(1): e8553. DOI: 10.1371/journal.pone.0008553.

82. Du L, Zhou Y, Jiang S. 2010. Research and development of universal influenza vaccines. *Microbes Infect* **12**: 280–286. DOI: 10.1016/j.micinf.2010.01.001.

83. Taborda CP, Juliano MA, Puccia R, Franco M, Travassos LR. 1998. Mapping of the T-cell epitope in the major 43-kilodalton glycoprotein of Paracoccidioides brasiliensis which induces a Th-1 response protective against fungal infection in BALB/c mice. *Infect Immun* **66**: 786–793.

84. Rothbard JB, Taylor WR. 1988. A sequence pattern common to T cell epitopes. *EMBO J* **7**: 93–100.

85. Yano A, Miwa Y, Kanazawa Y, Ito K, Makino M, Imai S, Hanada N, Nisizawa T. 2013. A novel method for enhancement of peptide vaccination utilizing T-cell epitopes from conventional vaccines. *Vaccine* **31**: 1510–1515. DOI: 10.1016/j.vaccine.2012.12.083.

86. Dayan FE, Daga PR, Duke SO, Lee RM, Tranel PJ, Doerksen RJ. 2010. Biochemical and structural consequences of a glycine deletion in the alpha-8 helix of protoporphyrinogenoxidase. *Biochim Biophys Acta* **1804**: 1548–1556. DOI: 10.1016/j.bbapap.2010.04.004.

87. Insaidoo FK, Borbulevych OY, Hossain M, Santhanagopolan SM, Baxter TK, Baker BM. 2011. Loss of T cell antigen recognition arising from changes in peptide and major histocompatibility complex protein flexibility: implications for vaccine design. *J Biol Chem* **86**: 40163–40173. DOI: 10.1074/jbc.M111.283564.

88. James EA, Moustakas AK, Bui J, Nouv R, Papadopoulos GK, Kwok WW. 2009. The binding of antigenic peptides to HLA-DR is influenced by interactions between pocket 6 and pocket 9. *J Immunol* **183**: 3249–3258. DOI: 10.4049/jimmunol.0802228.

89. Cárdenas C, Ortiz M, Balbín A, Villaveces JL, Patarroyo ME. 2005. Allele effects in MHC-peptide interactions: a theoretical analysis of HLA-DRbeta1*0101-HA and HLADRbeta1* 0401-HA complexes. *Biochem Biophys Res Commun* **330**: 1162–1167. DOI: 10.1016/j.bbrc.2005.03.102.

90. Painter CA, Cruz A, López GE, Stern LJ, Zavala-Ruiz Z. 2008. Model for the peptide-free conformation of class II MHC proteins. *PLoS One* **3**(6): e2403. DOI: 10.1371/journal.pone.0002403.

91. Benjamin DC, Berzofsky JA, East IJ, Gurd FRN, Hannum C, Leach SJ, Margoliash E, Michael JG, Miller A, Prager EM, Reichlin M, Sercarz EE, Smith-Gill SJ, Todd PE, Wilson AC. 1984. The antigenic structure of proteins: a reappraisal. *Annu Rev Immunol* **2**, 67–101. DOI: 10.1146/annurev.iy.02.040184.000435.

92. Madhumathi J, Prince PR, Anugraha G, Kiran P, Rao DN, Reddy MV, Kaliraj P. 2010. Identification and characterization of nematode specific protective epitopes of *Brugia malayi* TRX towards development of synthetic vaccine construct for lymphatic filariasis. *Vaccine* **28**: 5038–5048. DOI: 10.1016/j.vaccine.2010.05.012.

93. Benkirane N, Friede M, Guichard G, Briand JP, Van Regenmortel MH, Muller S. 1993. Antigenicity and immunogenicity of modified synthetic peptides containing D-amino acid residues. *J Biol Chem* **268**: 26279–26285.

94. Pandiaraja P, Arunkumar C, Hoti SL, Rao DN, Kaliraj P (2010) Evaluation of synthetic peptides of WbSXP-1 for the diagnosis of human lymphatic filariasis. *Diagn Microbiol Infect Dis* **68**: 410–415. DOI: 10.1016/j.diagmicrobio.2010.07.015.

95. Rudolph MG, Stanfield RL, Wilson IA. 2006. How TCRs bind MHCs, peptides, and coreceptors. *Annu Rev Immunol* **24**: 419–466 DOI: 10.1146/annurev.immunol.23.021704.115658.

96. Stavnezer J, Guikema JE, Schrader CE. 2008. Mechanism and regulation of class switch recombination. *Annu Rev Immunol* **26**: 261–292. DOI: 10.1146/annurev.immunol.26.021607.090248.

97. Smith-Garvin JE, Koretzky GA, Jordan MS. 2009. T cell activation. *Annu Rev Immunol* **27**: 591–619. DOI: 10.1146/annurev.immunol.021908.132706.

98. Lennon-Duménil AM, Bakker AH, Maehr R, Fiebiger E, Overkleeft HS, Rosemblatt M, Ploegh HL. Lagaudrière-Gesbert C. 2002. Analysis of protease activity in live antigen-presenting cells shows regulation of the phagosomal proteolytic contents during dendritic cell activation. *J Exp Med* **196**: 529–540. DOI: 10.1084/jem.20020327.

99. Delamarre, L, Pack M, Chang H, Mellman I, Trombetta ES. 2005. Differential lysosomal proteolysis in antigen-presenting cells determines antigen fate. *Science* **307**: 1630–1634. DOI: 10.1126/science.1108003.

100. Jemmerson, R., Paterson Y. 1986 Mapping epitopes on a protein antigen by the proteolysis of antigen-antibody complexes. *Science* **232**: 1001–1004. DOI: 10.1126/science.2422757.

101. Frazer J, Capra J. 1999. Immunoglobulins: structure and function. Fundamental immunology. Paul W. E (eds). Philadelphia-New York: Lippincott-Raven: 37–74.

102. Srivastava V, Yang Z, Hung IF, Xu J, Zheng B, Zhang MY. 2013. Identification of dominant antibody-dependent cell-mediated cytotoxicity epitopes on the hemagglutinin antigen of pandemic H1N1 influenza virus. *J Virol* **87**: 5831–5840. DOI: 10.1128/JVI.00273-13.

103. Gordon CL, Holmes NE, Grayson ML, Torresi J, Johnson PD, Cheng AC, Charles PG. 2012. Comparison of immunoglobulin G subclass concentrations in severe community-acquired pneumonia and severe pandemic 2009 influenza A (H1N1) infection. *Clin Vaccine Immunol* **19**: 446–448. DOI: 10.1128/CVI.05518-1164.

104. Larsen MV, Lundegaard C, Lamberth K, Buus S, Lund O, Nielsen M. 2007. Large-scale validation of methods for cytotoxic T-lymphocyte epitope prediction. *BMC Bioinf* **8**: 424. DOI: 10.1186/1471-2105-8-424.

105. He Y, Xiang Z, Mobley HL. 2010. Vaxign: the first web-based vaccine design program for reverse vaccinology and applications for vaccine development. *J Biomed Biotechnol* **2010**: 297505 DOI: 10.1155/2010/297505.

106. Sun J, Wu D, Xu T, Wang X, Xu X, Tao L, Li YX, Cao ZW. 2009. SEPPA: a computational server for spatial epitope prediction of protein antigens. *Nucleic Acids Res* **37**: W612–W616. DOI: 10.1093/nar/gkp417.

107. Schanen BC, De Groot AS, Moise L, Ardito M, McClaine E Martin W, Wittman V, Warren WL, Drake DR 3rd. 2011. Coupling sensitive in vitro and in silico techniques to assess cross-reactive CD4(+) T cells against the swine-origin H1N1 influenza virus. *Vaccine* **29**: 3299–3309. DOI: 10.1016/j.vaccine.2011.02.019.

108. Southwood S, Sidney J, Kondo A, del Guercio MF, Appella E, Hoffman S, Kubo RT, Chesnut RW, Grey HM, Sette A. 1998. Several common HLA-DR types share largely overlapping peptide binding repertoires. *J Immunol* **160**: 3363-3373.

109. Morris GM, Huey R, Olson AJ. 2008. Using AutoDock for ligand-receptor docking. *Curr Protoc Bioinformatics* Chapter 8: Unit 8.14. DOI: 10.1002/0471250953.bi0814s24.

110. Hess B, Kutzner C, Van der Spoel K, Lindahl E. 2008. GROMACS 4: algorithms for highly efficient, load-balanced, and scalable molecular simulation. *J Chem Theory Comput* **4**: 435–447. DOI: 10.1021/ct700301q.

111. Ciacci-Zanella JR, Vincent AL, Prickett JR, Zimmerman SM, Zimmerman JJ. 2010. Detection of anti-influenza A nucleoprotein antibodies in pigs using a commercial influenza epitope-blocking enzyme-linked immunosorbent assay developed for avian species. *J Vet Diagn Invest* **22**: 3–9. DOI: 10.1177/104063871002200102.

112. Rimmelzwaan GF, Baars M, Claas EC, Osterhaus AD. 1998. Comparison of RNA hybridization, hemagglutination assay, titration of infectious virus and immunofluorescence as methods for monitoring influenza virus replication in vitro. *J Virol Methods* **74**: 57–66. DOI: 10.1016/S0166-0934(98)00071-8.

113. Haste-Andersen P, Nielsen M, Lund O. 2006. Prediction of residues in discontinuous B-cell epitopes using protein 3D structures. *Protein Sci* **15**: 2558–2567 DOI: 10.1110/ps.062405906.

SUPPORTING INFORMATION

Additional supporting information may be found in the online version of this article at the publisher's web site.